# Model of Hyperthermia Therapy in Melanoma Treatment: Comparison between Constant and Temperature Dependent Blood Perfusion Rate

F. Ludin, and S.Yahud.
*School of Mechatronic Engineering, Universiti Malaysia Perlis (UniMAP),*
*02600 Arau, Perlis, Malaysia.*
*mohdnorfazly@gmail.com*

***Abstract*— This work deals with the modeling of hyperthermia therapy for melanoma skin cancer by considering 3D nonlinear Pennesbioheat transfer equation with Temperature Dependent Blood Perfusion Rate (TDBPR). The proposed model consists of a five-layer biological skin medium with third stage melanoma tumor utilizing each layer by Pennesbioheat equation. A Finite Element Analysis (FEA) in bioheat transfer model is employed and the result of nonlinear model in the time domains is solved using COMSOL Multiphysics. The variables of heat fluxes as control variables were applied to the proposed model for verification and assessing its applicability and effectiveness. The simulation output shows that the proposed model is valid under our test variable. This proposed model is used to easily and accurately study the thermal behavior of the biological skin during hyperthermia treatment procedure.**

***Index Terms*—Bioheat Transfer; Comsol Multiphysics; Melanoma; Simulation; TDBPR.**

## I. INTRODUCTION

Skin cancer happens when normal cells in the skin change into abnormal cells. There are two types of skin cancer; melanoma and non-melanoma [1]. Melanoma is a serious form of skin cancer. It happens when normal cells in the skin change into abnormal cells and grow out of control. Melanomas are classified into a number of stages from 0 to 4. Stage 0 means the melanoma cells are only in the top surface layer of skin cells. It is also called in situ melanoma. Stages 1 and 2 are the early stages, where the cancer was contained. In stage 3 it has spread to the lymph nodes. Stage 4 melanomas have spread elsewhere in the body, away from where it started [2].

Hyperthermia therapy is one of the treatments normally recommended to the patient with melanoma stage 3 and 4. In melanoma stage 3 and 4, the cancers have already reached the lymph nodes. Hyperthermia therapy is a cancer treatment that involves heating cells results in cell membrane damage, which, in turn, leads to the destruction of the cancer cells [3]. Hyperthermia treatment planning is an important therapeutic option in biomedical cancer medicine. It is a promising method to treat various types of cancer by heating the tumor tissue to about $42^{O}$C using various types of heating, thereby inducing preferential apoptosis of cancerous cells [4].

Hyperthermia dosing standardization is still a significant problem [5], [6]. Everybody agrees that hyperthermia treatment is an overheating of the targeted tissue, but unnecessary high temperature can dangerously overheat the healthy tissue, causing unwanted burn and necrosis [7]. Prediction of tissue temperature distribution in biological systems is required in hyperthermia therapy to optimize the amount of heat applied. A numerical simulation of bioheat transfer can be useful for prediction assessment of thermal dosimetry and exposure. Other than that, invasive measurement of temperature distribution may involve amounts of cost due to the complicated procedure, hospital stays, and also its theoretical solution is very difficult in real tissue structure due to its complex geometry and loading condition.

In this project, a transient heat transfer model of biological skin with melanoma during superficial hyperthermia treatment will be optimized. The model consists of a five-layer biological medium composed of stratum corneum, stratum germinativum, papillary layer, reticular layer, and subcutaneous tissue. A third stage melanoma tumor is introduced in the skin model. The Pennes Bioheat Equation is used to calculate the temperature distribution which the perfusion rate is assumed to be a function of temperature. It is called as Temperature Dependent Blood Perfusion Rate (TDBPR). This investigation has the capability to optimize the cancer hyperthermia therapy parameters and able to deal with many practical bioheat transfer problems.

## II. METHODOLOGY

### A. The Bioheat Model

The Equation (1) that Pennes [8] utilized is summarized as follows, in its three dimensional form:

$$\rho C \frac{\partial T}{\partial t} = k \frac{\partial^2 T}{\partial x^2} + k \frac{\partial^2 T}{\partial y^2} + k \frac{\partial^2 T}{\partial z^2} + \omega_b \rho_b c_b (T_a - T) + Q_m + Q_r(x, y, z; t) \quad (1)$$

where, T ($^0$C) is the local tissue temperature; $T_a$ ($^0$C) is the arterial temperature; $c_b$ (J/kg/$^0$C) is the blood specific heat capacity; $C$ (J/kg/$^0$C) is the tissue specific heat capacity; W (kg/m$^3$/s) is the local tissue blood perfusion rate; k (w/m/$^0$C) is the tissue thermal conductivity; $\rho$ (kg/m$^3$) is the tissue density; $Q_r$ (W/m$^3$) is the energy deposition rate; and $Q_m$ (W/m$^3$) is the metabolism, which is usually small compared to the external power deposition term $q_p$ [6].

The initial temperature of the skin is obtained through the solving of Pennes Bioheat equation. The three-dimensional form of temperature at initial condition is shown in Equation (2). $To$ is assigned as a constant initial condition at $t = 0\ s$.

$$T(x, y, z; 0) = T_0(x, y, z) \quad (2)$$

Another assumption that made for the initial condition is shown in Equation (3), where the external heat energy is stated as 0 W/m$^2$. This indicates that there is no external heat source applied to the skin during initial conditions, $t = 0\ s$.

$$Q_r(x, y, z; 0) = 0 \tag{3}$$

The Equation (1) becomes,

$$0 = k\frac{\partial^2 T}{\partial x^2} + k\frac{\partial^2 T}{\partial y^2} + k\frac{\partial^2 T}{\partial z^2} + \omega_b \rho_b c_b (T_a - T) + Q_m \tag{4}$$

The$z$ axis is ranged from 0 to L, where $L$ is a depth along the z axis, the initial temperature of the skin is equal to the body core temperature, $Tc$.

And when $z = Lmax$ , on the surface of the skin.

$$-k\frac{\partial T}{\partial n} = h_0[T_f - T_0(x, y, z)] \tag{5}$$

Where $h_0$ is the heat convection coefficient between the skin surface and the surrounding air temperature, and $T_f$ is the surrounding temperature [9].

In the case of hyperthermia treatment, the boundary condition of the skin is set as follows:

At $z = Lmax$ or at the surface of the skin the energy from its source is applied as presented in Equation (6).

$$-k\frac{\partial T}{\partial n} = f(x, y, z, t) \tag{6}$$

Where, $f(x, y, z, t)$ is the time dependent external heat source. When $z$ range from 0 to L or along the depth of the skin medium,

$$T = T_C \tag{7}$$

Considering that the biological body, tends to keep its core temperature to be in the normal state.

At the side and bottom surfaces, no heat flow occurs along these surfaces, assuming that the tissue distant from the area of interest is not affected by the imposed thermal disturbance [10]. Therefore, the thermally insulated condition of these surfaces is given by

$$-k\frac{\partial T}{\partial n} = 0 \tag{8}$$

*B. The Simulation*

The three-dimensional rectangular skin model (5 layers) with embedded third stage melanoma tumor is taken into consideration here. Each skin layer is assumed to be having different heat parameters. In the model displayed in Figure 1, the upper surface of the skin tissue is subjected to the several temperature settings. All sides and bottom surface boundary are treated as adiabatic boundaries by assuming the tissue remote from the area of interest is not affected by imposing thermal disturbance [11]–[13]. Also in Figure 2 Cartesian rectangular coordinate system is established and z denotes the tissue depth from the lower to the upper skin surface. The length and the width of the model are both 50mm. The thickness of each layer and its thermal properties are listed in Table 1.

Based on Figure 2 (b), the diameter of the tumor is 8mm. The tumor model is ulcerated on the skin surface by 1mm. The model is following the melanoma third stage cases. The tumor model is assumed to reached until lymph node location z=9.5mm or in the reticular region. That location is the interest location in melanoma stage 3 and 4 treatments, where the cancerous cell will metastasis to lymph nodes.

In hyperthermia practices, the treatment is performed using various types of applicators and placed on the surface of superficial tumors. In this simulation, the model is independent of the source type because heat energy is set on boundary setting on top of the skin(z=Lmax). Therefore, it can be flexibly used to calculate the temperature distribution for the various source type [4], [7], [14]–[17]. Furthermore, this model is capable of dealing with transient boundary condition and nonlinear source type.

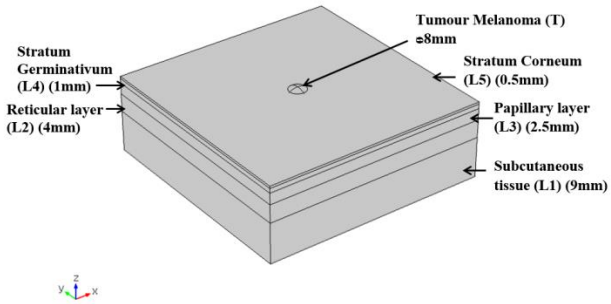


Figure 1: Three-dimensional multilayer skin model.

The thermal-physical properties of each skin layer from the literature[14]are employed in the computation. Table 1 and 2 shows the thickness and the properties for every each domain. The metabolic heat generation of skin and tumor is assumed to be different. Agnelli et al. reviewed that temperature at skin above a breast tumor or a malignant melanoma, a tumor of melanocytes which are found predominantly in skin, have been found to be several degrees higher than that of the surrounding area [18]. That happened because of the tumor has higher metabolic heat generation compared to surrounding skin.

The simulation software used in all simulations was COMSOL Multiphysics 5.0. The mode of study was set in the time-dependent problem. The solving time was set from 0 to 180-minute range with an increment of 1 second [19].

The skin model is initially kept at a constant or normal temperature. The computation is done for skin with and without tumor. The skin surface is set with natural convectional of environmental (T=25$^0$C, $h_0$=7W/m$^2$K) for 30s. In the normal condition, the rate of blood perfusion is assumed to be constant. This is the most used method given as [20]:

$$\omega_b = 5E^{-4}e^{0.0001T} \tag{9}$$

Without external heating, convection heat transfer coefficient has been found to have little effect on skin temperature. So the ambient convection coefficient is assumed to be 7 W/m$^2$K.

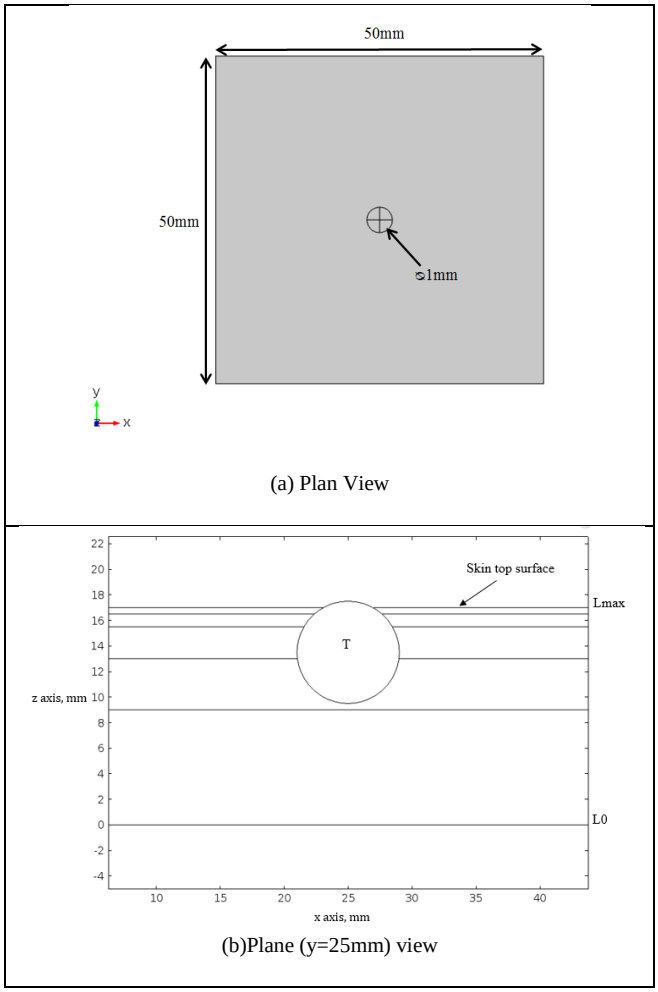


Figure 2: Model view (a) Plan view and (b) zx-plane view of the model.

In this study, the proposed numerical model is applied to several test variables for verifying and assessing its applicability and effectiveness. The values of the heat fluxes employed in the following analysis as test variables are listed in Table 3.

The constant heats are subjected on the surface of the skin. The duration of heat applied is depending on the amount of heat applied on top of the skin surface. In hyperthermia therapy, low amount of heat applied required a longer duration of heat application. In this work, the simulation time is assigned as the longest therapy time in practical t=180 minutes in all cases. In this simulation, the rate of blood perfusion is treated as a constant value and an exponential function to evaluate the simulation effect of temperature blood perfusion rate.

The other boundary and parameters setting is similar as in normal condition. Each simulation runs until t=180 minutes. The computation time is based on the longest duration of hyperthermia treatment. The ambient temperature and ambient convection coefficient are ignored because in this simulation, it is assumed to have no gap between the energy source pad and skin surface [21].

## III. Result and Discussion

### *A. Normal Condition*

In the normal condition, the result shows the effect of ambient temperature and ambient convection coefficient at the top of the skin surface (z=Lmax) to the skin medium (z=0 to z=L) before the application of external heat during superficial hyperthermia therapy. The two-dimensional thermal distribution for normal condition, skin with tumor and without tumor is shown in Figure 3. It shows that, the temperature at a reticular layer is slightly affected by ambient temperature and convection coefficient. The temperature is dropped from 37$^{O}$C to 34.5$^{O}$C near the skin surface while another area is maintained constant with core body temperature 37$^{O}$C.

Table 1
Thermal Properties of Each Domain[20], [11].

| Description | Thickness, L (mm) | Thermal conductivity k ($Wm^{-1}K^{-1}$) | Density P ($kgm^{-3}$) | Specific heat, c ($Jkg^{-1}K^{-1}$) |
|---|---|---|---|---|
| Subcutaneous Tissue (L1) | 9.0 | 0.185 | 971 | 2700 |
| Reticular Layer (L2) | 4.0 | 0.445 | 1116 | 3300 |
| Papillary Layer (L3) | 2.5 | 0.445 | 1116 | 3300 |
| Stratum Germinativum (L4) | 1.0 | 0.235 | 1190 | 3600 |
| Stratum Corneum (L5) | 0.5 | 0.235 | 1190 | 3600 |
| Tumor (T) (melanoma stage 3 or 4) | 8.0 | 0.558 | 1030 | 3700 |

Table 2
Constant Parameter of Skin and Tumor[20].

| Parameters | Value |
|---|---|
| Blood density (kg/m3) | 1060.0 |
| Blood specific heat (J/kg/ | 3770.0 |
| Metabolic heat generation of skin, W/m$^2$ | 368.1 |
| Metabolic heat generation of the tumor, W/m$^2$ | 450 |
| Constant blood perfusion rate, $\omega_b$, 1/s | $5E^{-4}$ |
| Temperature dependent blood perfusion, $\omega_b$, 1/s | $5E^{-4}e^{0.0001T}$ |
| Arterial Blood temperature ($^0$C) | 37 |
| Core Temperature ($^0$C) | 37 |

Table 3
Test Variable For Boundary Condition[3], [22].

| Test Variable | Values |
|---|---|
| Constant Heat Flux, $f(x,y,z,t)$, W/m$^2$ | 110 |
| | 130 |
| | 160 |
| | 200 |

At z=8mm, the temperature starts to decline gradually. It indicates that the surrounding condition managed to affect up to reticular layer. Comparison of temperature plot along z-axis was made to identify the temperature difference between skin with and without tumor, as shown in Figure 4. The temperature plot at z=17mm for a skin model with the tumor is 35.5 $^0$C whereas for the model without tumor is 34.1 $^0$C. The temperature difference at z=17mm is about T=1.4$^0$C. It also shows that at z≈11.5mm, the plot between two skin

models started to show different temperature gradient. This is due to the difference in the metabolic heat rate of skin and tumor tissue.

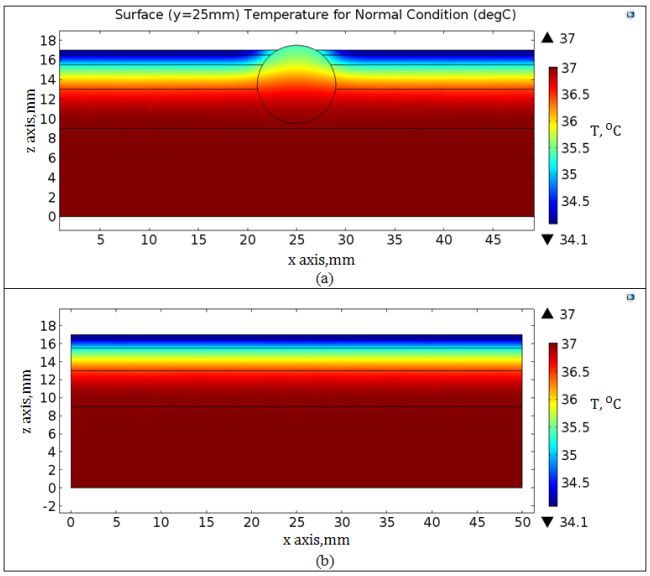


Figure 3: Surface contour plots at zx-plane (a) skin with melanoma tumor and (b) skin without tumor.

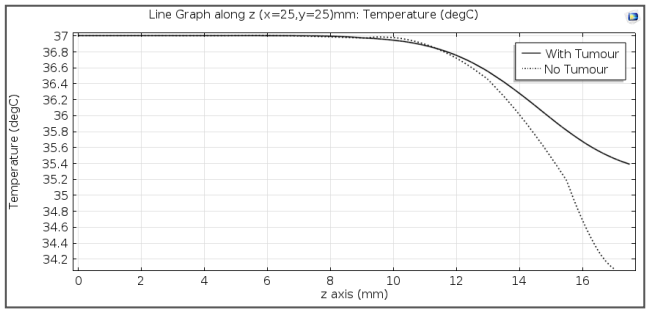


Figure 4. Temperature plots along the z-axis for normal condition (with and without tumor).

Based on simulation output, we found the influence of ambient temperature and convection heat transfer coefficient in the skin temperature. This found valid the conclusion made by Feng et al. that using modified Pennes Equation and linear biological tissue model as their study [12]. We also found that there is a temperature difference between skin with and without tumor because of the difference thermal-parameters of tumor and skin. This is also found by Freitas et al. that using parallel computation GPU to analyze a non-linear 3D heterogeneous model to study the temperature increase [23].

### *B. Test Variable*

In this part of the simulation, the effect of constant heating on skin temperature is studied. Figure 5 and 6 shows the simulation output. The skin surface temperature is ranging from 42.2$^{O}$C to 46.1$^{O}$C. The maximum temperature plot at t=180 minutes for heat 110 W/m$^2$ is 42.2$^{O}$C, 130 W/m$^2$ is 43.1$^{O}$C, 160 W/m$^2$ is 44.5$^{O}$C, and 200 W/m$^2$ is 46.3$^{O}$C. The larger amount of heating, the higher local temperature plot at the skin surface.

Temperature plot in Figure 5 shows the temperature gradient at t=180 minutes along the depth of skin. At depth 9.5mm the temperature had small change. This is because of the different heat metabolism of skin and tumor. The relative between normal and all external heat applied is depicted in Figure 6. It shows the temperature at z=9. 5mm is increased when the amount of heat applied to the surface of the skin is increased. This information is useful for thermal comfort evaluation during hyperthermia treatment. The applied heat flux values during hyperthermia procedure can be chosen based on the safe range of the biological skin. Generally, long duration and high surface heating will cause pain even burning to the skin tissues.

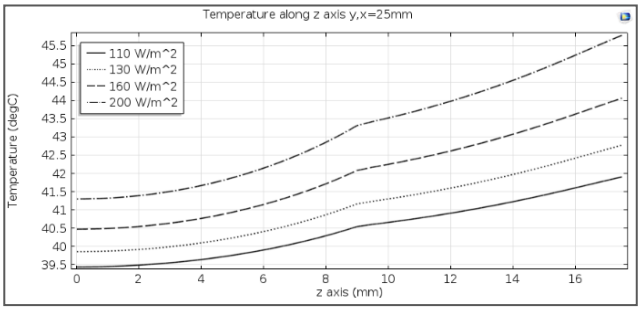


Figure 5: Temperature plot along the z-axis (t=180 min) for different heat fluxes.

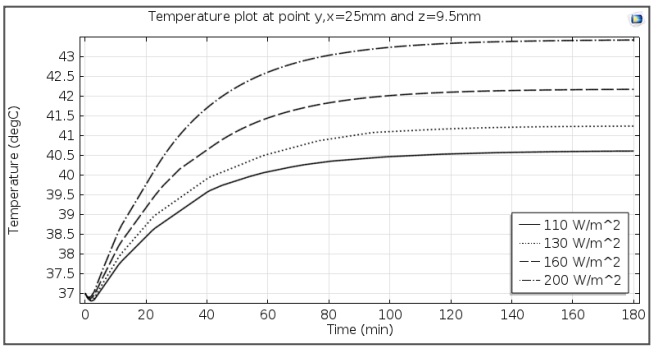


Figure 6: Temperature plot for different heat fluxes.

Figure 6 shows the temperature plotted at point x=25mm, y=25mm and z=9.5mm. For comparison between all four subjected heats, the plot is taken until t=180 minutes. For heat 200 W/m$^2$, the temperature was settled at t=120 minutes. Compared to other heat applied, 200 W/m$^2$temperature settle take longer time. For heat 160 W/m$^2$ temperature settle is T=42.1$^{O}$C at t=110 minutes, heat 130 W/m$^2$ temperature settle is T=41.3$^{O}$C at t=105 minutes and heat 100 W/m$^2$ temperature settle is T=40.1$^{O}$C at t=100 minutes.

During hyperthermia therapy, the heat subjected on the skin surface may kill or weaken the cancer cells in the lymph node regions. The cancerous cells can be killed at temperature 42$^{O}$C. From the temperature plot in Figure 6, heat flux 160 W/m$^2$ and 200 W/m$^2$ are the heat applied that possible to kill the cancer cells at 100 minutes and 43 minutes respectively [15].

The second part is the simulation when temperature dependent blood perfusion rate is considered in the computation. The blood perfusion rate changes exponentially when the local temperature is changing. The simulation result shows in Figure 7 and 8 is the comparison of temperature plots between constant and temperature dependent blood perfusion rate.

In Figure 7, the temperature plot started to show the difference when the local temperature reached a certain time. For 110 W/m$^2$ heat applied, the model with TDBPR had a lower temperature (0.2$^{O}$C) then the model with constant blood perfusion when t=100 minutes. Similar to 200 W/m$^2$

heat applied, the difference of local temperature in TDBPR model and constant blood perfusion is started at t=50 minutes. Figure 8 represents the temperature plot along the z-axis at t=180 minutes. It shows all local temperature for every heat applied had about 0.2$^{O}$C -0.3$^{O}$C different between TDBPR model and constant blood perfusion model.

It shows the effects of TDBPR on the temperature plot at lymph node location. The plot graph shows the exponential form produced the highest tissue temperature and the quadratic form shows the lowest tissue temperature. Zhang et al. and Sun et al. are the authors that deal with TDBPR in their models with different methods and assumptions [14], [12]. They found that the TDBPR gave an influenced to the simulation results and agreed that TDBPR are important parameters for predicting the temperature in bioheat problems.

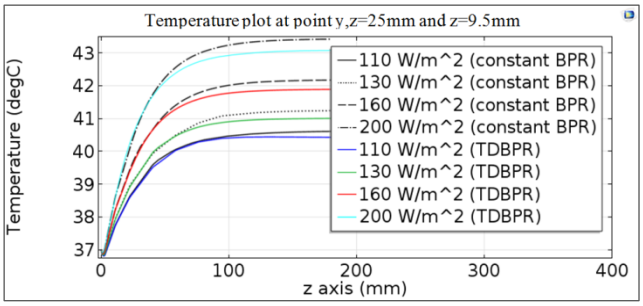


Figure 7: Temperature plots for constant blood perfusion rate and temperature dependent blood perfusion rate.

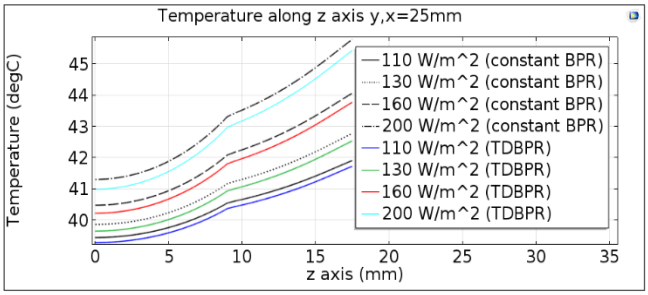


Figure 8: Temperature plots along the z-axis (t=180 min) for constant blood perfusion rate and temperature dependent blood perfusion rate.

## IV. Conclusion

The linear and nonlinear transient heat transfer model of biological skin during superficial hyperthermia for melanoma treatment is considered. The nonlinearity of the model is due to the temperature dependence of the blood perfusion rate. A bioheat equation based on hyperthermia problems is introduced in the proposed model. In the simulation for normal condition, the ambient temperature and convection coefficient were affecting the temperature gradient of the skin. The presence of tumor in a skin model is something necessary because it has difference in metabolic heat generation. Blood perfusion in temperature calculations should be treated as temperature dependent quantity. Next, a test variable is employed in the model to verify the developed model and the results show the model is reliable to use in predicting the temperature distribution in melanoma skin cancer during hyperthermia therapy.

These results are expected to be valuable for clinical tumor treatments. In treatment planning of tumor hyperthermia, this research can also be used to achieve complete tumor destruction and minimal surrounding tissue damage. The amount of tissue damage based on heat applied will be put as a consideration in our next work.

## References

[1] B. Friedrich, "Modeling melanoma, Drugs Disc.", Elsevier, vol. 3, no. 2., 2006.
[2] K. A. Beaumont, N. Mohana-kumaran, and N. K. Haass, "Modeling melanoma in vitro and in vivo," J. Healthc., no. 2, pp. 27–46, 2014.
[3] C. W. Song, "Effect of local hyperthermia on blood flow and microenvironment :A review," Cancer Res., vol. 44, no. October, pp. 4721–4730, 1984.
[4] C. Thomas, C. William, D. Evans, and H. Fred, "Hyperthermia treatment planning," Am. Assoc. Phys. Med., vol. 27, no. August, pp. 1–57, 1989.
[5] M. W. Dewhirst, "Basic principles of thermal dosimetry and thermal thresholds for tissue damage from hyperthermia," Int. J. Hyperth., no. May, pp. 267–294, 2009.
[6] R. B. Roemer, B. R. Paliwal, F. W. Hetzel, and M. W. Dewhirst, "Heat transfer in hyperthermia treatments: basic principles and applications," Biol. Phys. Clin. Asp. Hyperth., pp. 210–242, 1988.
[7] C. Erik, D. G. Bouche, and D. jacobi van der Zee, "Hyperthermia in cancer treatment," Reliab. cancer Ther., vol. 1, no. 2, pp. 1–48, 2011.
[8] H. H. Pennes, "Analysis of tissue and arterial blood temperatures in the resting human forearm," J. Appl. Physiol., vol. 1, no. 2, 1948.
[9] D. Derome, B. Blocken, and J. Carmeliet, "Determination of surface convective heat transfer coefficients by CFD," vol. 1, no. 2, 2007.
[10] J. Vlachopoulos and D. Strutt, "Basic heat transfer and some applications in polymer," Plast. Tech. Toolbox, vol. 2, pp. 21–33, 2002.
[11] Z. Zhang, "Transient bioheat transfer analysis in biological tissues by fundamental-solution-based numerical methods," Mol. Cell. Biomech., vol. 1, no. March 2015, pp. 31–53, 2013.
[12] F. Sun, A. Chaney, R. Anderson, and G. Aguilar, "Thermal modeling and experimental validation of human hair and skin heated by broadband light," Laser Surg. Med., vol. 169, no. December 2008, pp. 161–169, 2009.
[13] D. Zhong-Shan and L. Jing, "Mathematical modeling of temperature mapping over skin surface and its implementation in thermal disease diagnostics," Comput. Biol. Med., vol. 34, no. June, pp. 495–521, 2004.
[14] Z. Zhang, H. U. I. Wang, and Q. Qin, "Method and fundamental solutions for nonlinear skin bioheat model," J. Mech. Med. Biol., vol. 14, no. 4, 2014.
[15] R. W. Y. Habash, R. Bansal, D. Krewski, and H. T. Alhafid, "Thermal therapy , part 2 : Hyperthermia techniques," Crit. Rev. Biomed. Eng., vol. 34, no. 6, pp. 491–542, 2006.
[16] B. Yngve, J. Svein, M. Paolo, and S. Paul, "Flow patterns and heat convection in a rectangular water bolus for use in superficial hyperthermia," Phys. Med. Biol., vol. 13, no. July, pp. 3937–3953, 2009.
[17] D. Sardari and N. Verga, "Cancer treatment with hyperthermia," Curr. cancer Treat. beyond Conv. approaches, 2006.
[18] J. P. Agnelli, A. A. Barrea, and C. V Turner, "Tumor location and parameter estimation by thermography," Math. Comput. Model., vol. 53, no. 7–8, pp. 1527–1534, 2011.
[19] R. W. Pryor, Multhyphysics modelling using COMSOL-A first principles approach. Sudbury, Massahusetts: Jones and Bartlett Publishers, 2011.
[20] T. Igarashi, K. Nishino, and S. K. Nayar, "The appearance of human skin," Ski. Care Res., pp. 8–16, 2005.
[21] H. Huang and Horng Tzyy-Leng, Bioheat transfer and fluid flow in biological process, no. January. London NW1 7BY, UK: Elsevier, 2015.
[22] Z. Deng and J. Liu, "Analytical study on bioheat transfer problems with spatial or transient heating on skin surface," J. Biomech. eng., vol. 124, no. December, pp. 638–649, 2002.
[23] R. Freitas, S. Loureiro, and M. Lobosco, "3D numerical simulations on GPUs of hyperthermia with nanoparticles by a nonlinear bioheat model," J. Comput. Appl. Math., vol. 295, pp. 35–47, 2016.